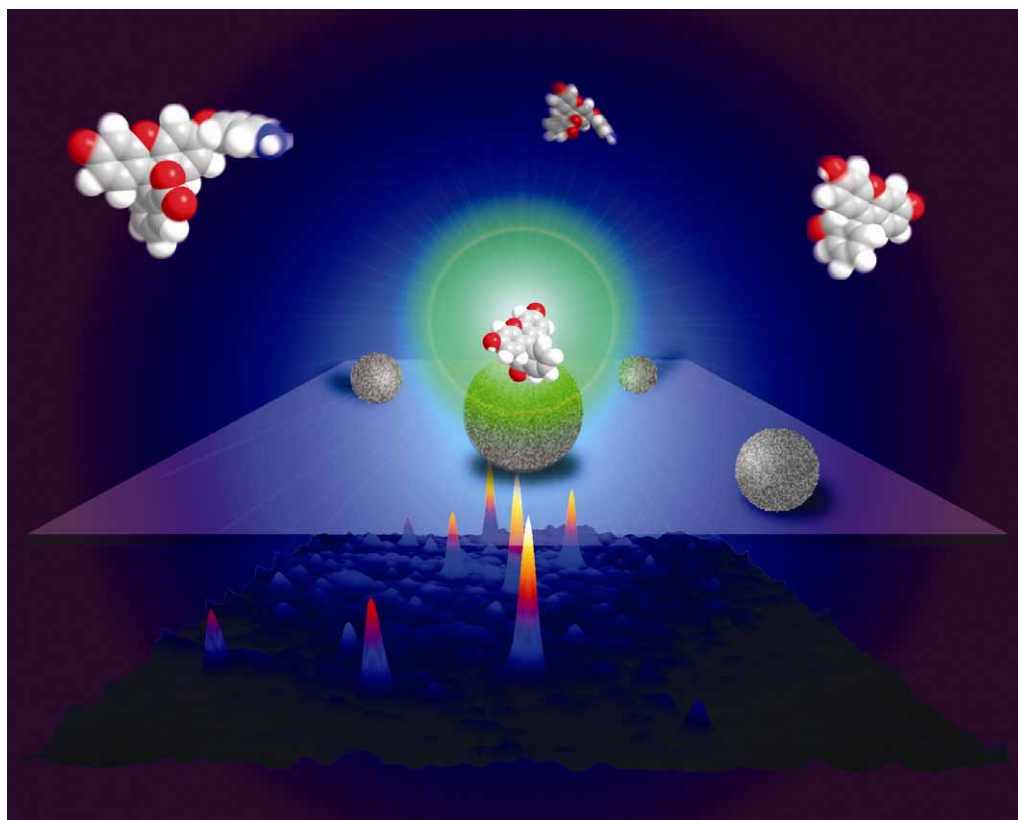


# Chem Soc Rev

This article was published as part of the  
*In-situ* characterization of heterogeneous  
catalysts themed issue

Guest editor Bert M. Weckhuysen

Please take a look at the issue 12 2010 [table of contents](#) to  
access other reviews in this themed issue



# Reporters in the nanoworld: diffusion of single molecules in mesoporous materials†

Jens Michaelis\* and Christoph Bräuchle\*

Received 14th September 2010

DOI: 10.1039/c0cs00107d

Mesoporous materials have a high potential for a number of different applications in Materials Science such as in molecular sieving, as masks for the formation of nanometre-sized metallic wires, as novel drug-delivery systems or as advanced host systems for catalysis. For many of these applications a thorough understanding of the interaction of guest molecules within the host matrix is required. In this *tutorial review*, we cover recent single-molecule experiments that allow the investigation of host–guest dynamics with unprecedented detail. We will show how molecules diffusing in samples with (almost) perfect domain ordering still show a large heterogeneity in their mobility and interaction with the host. With the presented methodology it is now possible to dramatically improve our understanding of host–guest interactions and in return develop new nano-structured mesoporous materials with properties optimised for a certain application.

## Introduction

Through self-assembly of surfactants and framework building blocks a variety of periodic mesoporous silica structures can form spontaneously.<sup>1–4</sup> Due to their large surface area, tunable pore diameter and chemically modifiable surfaces these materials are of ever growing interest for novel nano-technological applications such as molecular sieving,<sup>5</sup> catalysis,<sup>6</sup> novel drug-delivery systems,<sup>7,8</sup> as matrices for carbon casting or for the stabilisation of conducting nanoscale wires.<sup>9</sup> For most of these applications it is of utmost importance to investigate and control the mobility of guest species loaded into the host material. While methods such as pulsed field

gradient NMR<sup>10</sup> provide a good overview about the average mobility, it is clear that the formation of such nano-structured environments will lead to large structural heterogeneities. These heterogeneities will in turn result in different interactions of guest molecules within the host material and this will in return lead to dynamic heterogeneities of guest molecule diffusion. Therefore, in order to optimise host–guest systems methods are required that can resolve these heterogeneities in a spatial and temporal manner. This becomes possible when using fluorescent molecules as guests at ultra-low concentrations,<sup>11–14</sup> such that their movement can be followed by single-molecule experiments. Localisation of single molecules can be performed, a technique termed single-molecule imaging,<sup>15</sup> thus allowing for the observation of the diffusion behaviour of a single-molecule within the complex surrounding of a nanochannel network.

In the following we will give an overview of experiments performed in the last five years characterising the diffusion of molecules in mesoporous materials of different topologies and different surface functionalities. In addition we will report on

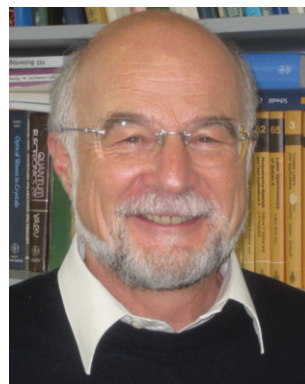
*Department of Chemistry and Center for Nanoscience (CeNS), Ludwig-Maximilians-Universität München, Butenandstr. 11, 81377 München, Germany. E-mail: michaelis@lmu.de, christoph.braeuchle@cup.uni-muenchen.de*

† Part of the themed issue covering recent advances in the *in-situ* characterization of heterogeneous catalysts.



Jens Michaelis

*Jens Michaelis is an Assistant Professor at the LMU Munich. After receiving his PhD in Physics in 2000, he spent several years as a Postdoc at the University of California, Berkeley, focusing on single-molecule studies of molecular motors. His research interests are the molecular mechanisms that underlie the biological activity of proteins and mechanical properties of polymer molecules. In 2007 he was awarded the Römer Prize from the LMU for his habilitation work and in 2010 he received the Nernst-Haber-Bodenstein Award.*



Christoph Bräuchle

*Christoph Bräuchle is Professor at the Ludwig-Maximilians-University Munich. After his PhD, he spent one year as a postdoc at IBM in San José, California, USA. His research focuses on imaging, spectroscopy and manipulation of single molecules in bio- and nano-sciences. Besides numerous publications in international journals, Prof. Bräuchle has won several honors, including the Philip Morris Research award and the Karl Heinz Beckurts Prize 2002. He is also a member of the Academia Europaea.*

the influence of different solvents as well as that of bulky side-groups to the diffusion properties of the dye molecules.

## Nano-structured silica materials

Mesoporous silicas exist in various forms albeit in this review we will concentrate on thin films which are prepared *via* cooperative self-assembly of surfactant molecules with polymerizable silicate species in a process termed evaporation induced self assembly.<sup>16</sup> As reporters for the environment within these films strongly fluorescent molecules such as *e.g.* terrylenediimide (TDI) molecules, a bright and photostable dye,<sup>17–19</sup> (Fig. 1a) can be added at very low concentrations to the synthesis solutions of the mesoporous films. Thus, dye molecules can be incorporated into the nanometre sized channels during the evaporation-induced self-assembly of the material in the spin-coating process. Film thickness can be fine-tuned by modifying rotation speeds as well as solvent content resulting in silica films with a thickness between roughly 50–500 nm. An interesting aspect of these materials is that by varying the molar ratio between the surfactant and

the silica oligomers of the precursor solution, materials with different mesopore topologies can be prepared (Fig. 1). A low surfactant to silica ratio will result in a hexagonally ordered mesophase whereas using a high surfactant to silica ratio a lamellar mesophase can be prepared (Fig. 1c). Interestingly, if one uses an intermediate mixture one can find conditions where the two mesophases coexist in the same sample. Later in this review, we demonstrate that these topologies in fact strongly influence the diffusion of the molecules inside the pores.

Characterization of these structures is typically done by analyzing X-ray diffraction (XRD) patterns (Fig. 1b) and TEM cross-section images<sup>1</sup> (Fig. 1d). The peak positions in the XRD patterns permit the calculation of the mean pore-to-pore distance. For the examples shown this distance is 6.1 ( $\pm 0.1$ ) nm for the lamellar phase and 6.3 ( $\pm 0.1$ ) nm for the hexagonal phase. These numbers correspond only to the average pore-to-pore distances, and the broadness of the peaks gives an indication of the actual distribution of pore-to-pore distances and pore sizes present in the samples. Typical wall thicknesses in these systems amount to about 1–2 nm, thus a

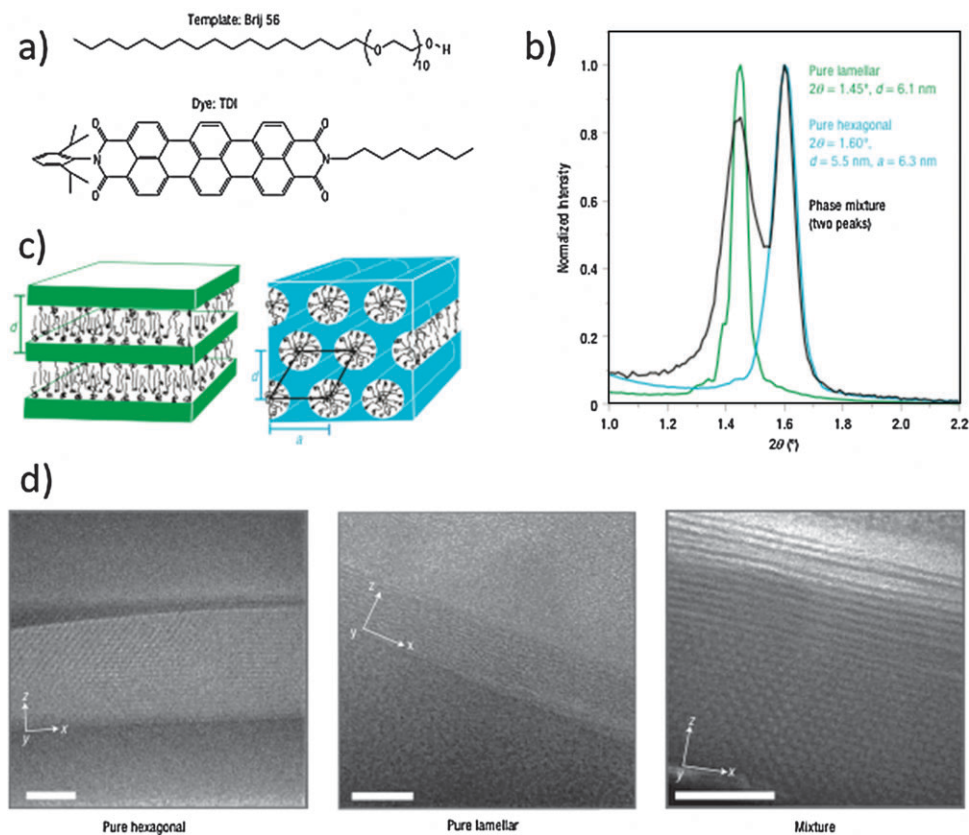


**Fig. 1** Mesoporous templated silica materials. (a) Structure-directing agent poly(oxyethylene) cetyl ether copolymer (Brij 56) and fluorescent terrylene diimide derivative (TDI), which are incorporated into the mesopores. (b) The small-angle X-ray diffraction patterns show the different peak positions for the lamellar (green) and the hexagonal (blue) phases. The two peaks in the diffractogram of the third sample (black) reveal the presence of the two phases present in the same film. The lamellar phase has a d-spacing of 6.1 nm; the hexagonal phase has a d-spacing of 5.5 nm (unit cell dimension  $a = 6.3$  nm). (c) Schematic diagrams of the lamellar and hexagonal pore topologies with the respective arrangement of the template inside the pores. (d) The cross-section TEM on the left clearly shows the openings of hexagonally arranged pores and the middle one shows the stacking of the lamellae. For the phase mixture (right), it shows the different mesophases stacked on top of each other. A different stacking order can be observed in other areas of this sample. In all of the images, the glass substrate is visible at the bottom and the silica–air interface is visible at the top, the arrows point along the optical axis of the wide-field microscope ( $z$  direction) in the observation plane ( $x$ – $y$  direction,  $y$  is pointing into the drawing plane). The scale bars represent 50 nm.<sup>20</sup>

pore diameter of 4–5 nm is filled with template and provides the space for molecular movement. TEM cross-sections on the other hand allow for a direct investigation of domain orientation and size. Unfortunately, the TEM images alone give no information about the real connectivity of the pores for molecules diffusing in them, since the TEM images give the average information over the whole thickness of the film, thus averaging the information from tens of layers. In order to get such direct insight into the interior network architecture a correlative approach of single-molecule tracking and electron microscopy is required.

### Mapping structural features using correlative electron microscopy and single molecule tracking

Because the molecular movement in the pore system is one of the most important and defining characteristics of porous materials, it is of interest to learn about this behaviour as a function of local structure. The combination of electron microscopic mapping and optical single-molecule tracking experiments reveal how a single luminescent dye molecule travels through linear or strongly curved sections of a mesoporous channel system whereby this curved section is part of the larger domain architecture of the sample. With this approach one can directly correlate porous structures detected by transmission electron microscopy with the diffusion dynamics of single molecules detected by optical microscopy. This opens up new ways of understanding the interactions of host and guest. For the implementation of this approach, key sample requirements include extremely thin mesoporous films which are both transparent for electrons and allow optical access. Moreover, specific markers have to be included which allow for the direct investigation of diffusion inside the silica channels and for a correlation between optical and transmission electron images of the sample. In the described experiments TDI molecules were used as molecular beacons for single-molecule tracking, polystyrene beads (280 nm in diameter) as markers that are visible in both transmission electron microscopy (TEM) and optical microscopy, and gold colloids (5 nm in diameter) for merging several electron micrographs. All these markers were added to the synthesis solution of the mesoporous film. The mesoporous film was spin-coated into the interior of a small micron-sized window within a thin ( $d = 30$  nm)  $\text{Si}_3\text{N}_4$  membrane which is supported by a small silicon wafer.

The combination of the two techniques provides the first direct proof that the molecular diffusion pathway through the pore system correlates with the pore orientation of the two-dimensional hexagonal structure (Fig. 2). In addition, the influence of specific structural features of the host on the diffusion behaviour of the guest molecules can be clearly seen. One can see in unprecedented detail, how a single fluorescent dye molecule travels through linear or strongly curved sections of the hexagonal channel system in a thin film of mesoporous silica, how it changes speed in the channel structure, and how it bounces off a domain boundary with a different channel orientation. Furthermore, one can show how molecular travel is stopped at a less ordered region, or how lateral motions between 'leaky' channels allow a molecule to explore

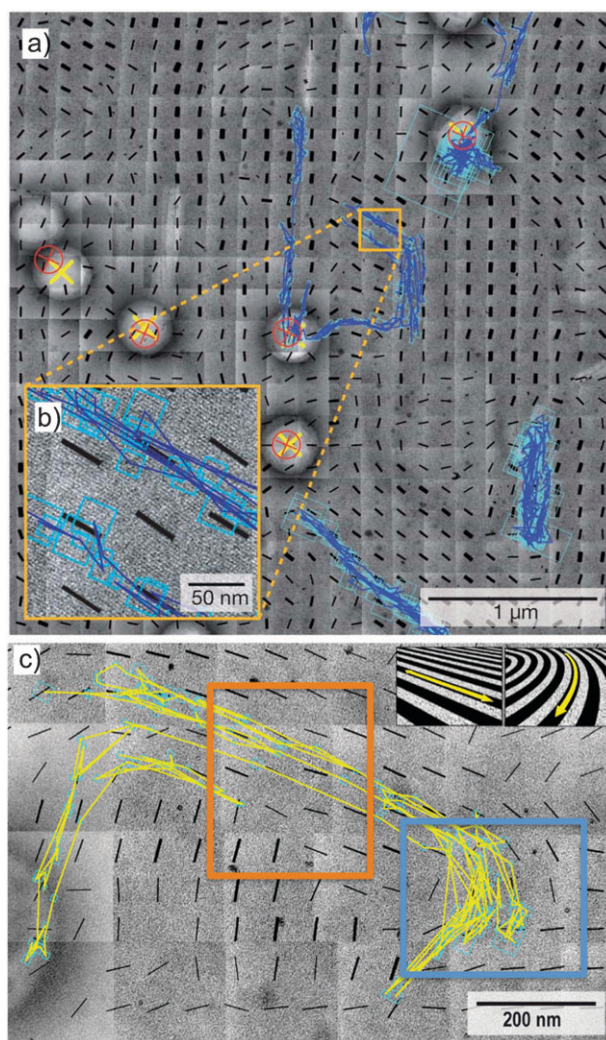


**Fig. 2** Overlay of single-molecule and TEM. (a) Shown are multiple TEM images of hexagonally ordered mesoporous silica films, templated with CTAB, stitched together to provide a macroscopic overview of the sample. Clearly visible are 5 polystyrene beads (centers indicated by yellow crosses) that were used as markers to correlate fluorescence and TEM images. Single-molecule imaging was used to follow the diffusion behaviour of individual TDI molecules embedded into the nanometre-sized channels of the mesoporous films. Extracted single-molecule trajectories are shown as an overlay (dark-blue lines) indicating also the computed accuracy of the position determination (cyan squares). A Fourier transform of the TEM images allows for the determination of the local orientation of the pores, which are indicated by black bars. The thickness of the bar is an indicator for the local order of the structure.<sup>20,28</sup> (b) Zoom into the TEM image. Now the orientation of the channels averaged over the thickness of the complete film can be seen also directly. The single molecule diffuses through two different parts of the same domain with a distinct spacing of about 100 nm, clearly above the measurement accuracy. (c) Another example of the TEM–single-molecule tracking overlay shows a good example of how the single-molecule trajectory is influenced by the domain architecture observed by the TEM images. While in the region highlighted by the orange square the molecule follows two different but parallel pathways, in a different area, a domain boundary leads to a dead-end and thus the resulting trajectory is curved (blue square).<sup>29</sup> The insets show cartoon representations of the described effects.

different parallel channels within an otherwise well-ordered periodic structure. This enormous heterogeneity of diffusional

behaviour only becomes apparent through the single molecule experiments.

An overlay of the TEM image, the extracted FFT directors which highlight the orientation of the structure (angle) as well as the degree of ordering (thickness) with the recorded single-molecule trajectories, shows a variety of the described structural features (Fig. 2). The positioning error for the single molecule trajectories is in the range of only 10–20 nm; the molecular positions can therefore be assigned to an ensemble of about five to ten parallel channels. Note, that while the single-molecule experiment describes the motion within a single nano-channel, the TEM image corresponds to an average over the thickness of the film, thus averaging over tens of channels. Thus, while the TEM overlay gives a good indication about the general local architecture it cannot show single defect sites, such as closed channels or openings to neighbouring channels. However, as we will show later, for certain samples it is possible to tune the time scale of diffusion such that the spatial accuracy of the single-molecule tracking technique can reach the single channel limit.

### Diffusion in the lamellar phase

Whereas the diffusion in the hexagonal phase is found to follow the underlying domain architecture of the mesoporous sample, the observed single-molecule trajectories in the lamellar phase appear completely unstructured (Fig. 3a), *i.e.* the molecule undergoes a free two-dimensional diffusion.<sup>20</sup> This can be understood since the silica layers have formed parallel to the sample surface and thus parallel to the field of view and diffusion within the image plane corresponds to a diffusion in the template filled layer. In addition diffusion is again quite heterogeneous and one can observe two different classes of diffusing molecules: One class of molecules exhibit a fast, totally unstructured diffusion.<sup>21</sup> The fluorescence recorded from these molecules appear with the typical Gaussian-shaped diffraction patterns (Fig. 3b). This is consistent with the random motion in the surfactant layers between the silica planes which allows two-dimensional diffusion. The other class of molecules show a much slower diffusion (difference in diffusion coefficients  $10^3$ ). In addition, the fluorescence recorded from this second class of molecules appear as doughnuts (Fig. 3c). Such doughnut-shaped diffraction patterns can be assigned to single molecules whose transition dipole moment (for the TDI dye molecule used in these studies this corresponds to the long molecular axis) is constantly aligned along the optical axis of the microscope. This means that these molecules are oriented perpendicular to the glass substrate and thus normal to the silica planes of the lamellar phase. The doughnuts move in a random way similarly to the Gaussian-shaped molecules, however, the diffusion is much slower (Fig. 3d).

Why would some of the molecules show one *versus* another orientation within the lamellar phase? Strong interactions between the dye molecules and the template molecules, could result in the alignment of the molecules along the template chains, *i.e.* perpendicular to the silica layers. In contrast, if for a different class of molecules these interactions are not strong enough to be able to orient the molecules, the molecules are able to take different orientations within the surfactant-filled

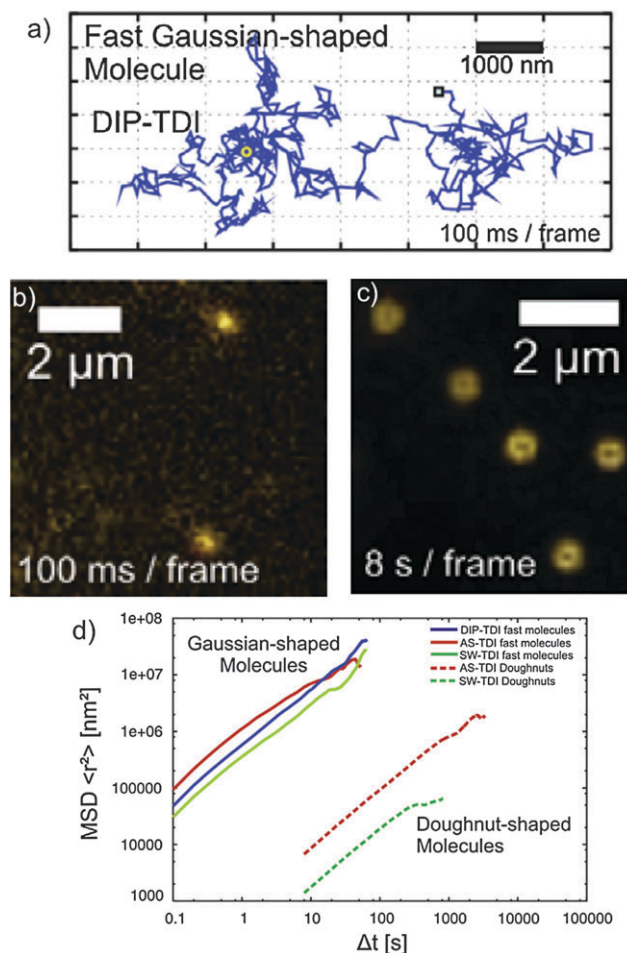


**Fig. 3** Observed fluorescence patterns and diffusion rates. (a) Single-molecule trajectory of a DIP-TDI molecule diffusing through the lamellar phase. The trajectory is completely unstructured showing free 2-dimensional diffusion, as expected for the lamellar phase. (b) Fluorescence emission pattern of molecules in the lamellar phase showing fast, unstructured diffusion. The observed patterns can be well described with two-dimensional Gaussian intensity distributions, as expected for the emission from a point object. (c) Emission pattern from slowly diffusing molecules. The intensity distribution shows a donut like shape, as expected for molecules with a fixed transition-dipole orientation perpendicular to the image plane. (d) Overview of the MSD for dye-molecules showing Gaussian-shaped or donut like fluorescence emission patterns. Note, that the former molecules diffuse much faster than the latter.<sup>21</sup>

layers. This hypothesis was verified by testing TDI molecules with different tails (Fig. 4). While no doughnut at all could be observed with DIP-TDI a symmetric TDI molecule with two 2,6-diisopropyl-phenyl substituents, AS-TDI molecule, where one of the 2,6-diisopropyl-phenyl substituents was replaced by an octyl tail, exhibit about 90% doughnuts, and in the case of SW-TDI, a molecule with two 1-heptyl-octyl substituents, a ratio of about 1:1 for the two populations was observed.<sup>21</sup> Interestingly, transitions between the sub-populations could even be observed for AS-TDI as well as for SW-TDI. Such switches transforming fast Gaussian-shaped molecules into slow doughnuts and the other way round are encountered occasionally. They indicate a sudden change in the orientation

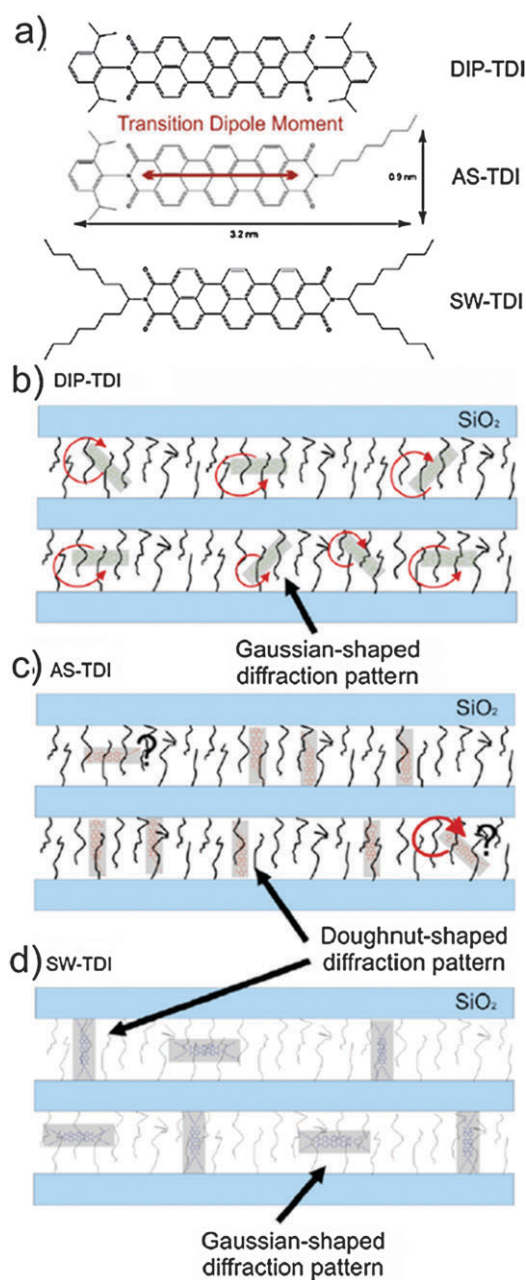


**Fig. 4** Molecular picture for diffusion in the lamellar phase. (a) Structure of the three different TDI derivatives whose diffusion in the lamellar phase was investigated. (b)–(d) Cartoons indicating the observed behavior for DIP-TDI, AS-TDI and SW-TDI respectively.<sup>21</sup>

of the molecules accompanied with a dramatic change in the diffusion coefficient.

The emerging picture of the behaviour of the three TDI-dyes in the lamellar structure is that DIP-TDI molecules do not keep a preferential orientation, but constantly reorient during their walk within the template-filled lamellas. In this system the host–guest interactions are relatively weak and do not influence the orientation of the DIP-TDI molecules significantly. In contrast, 90% of the AS-TDI molecules align along the template molecules due to strong interactions, and diffuse slowly in this configuration appearing as doughnuts. The other 10%, the fast Gaussian-shaped molecules, may

rotate freely, similarly to DIP-TDI. Finally, the SW-TDI molecules are found in both of the two distinct orientations with about equal probability. Strong interactions between the four alkyl tails of SW-TDI and the template molecules dictate these two preferential configurations. Moreover, switches between these two populations can occur, as already mentioned. This shows that although the two populations refer to two energetically favoured orientations, the molecules are able to overcome the energetic barriers occasionally, maybe at defect sites in the silica walls or in the template of the host structure.<sup>21</sup>

### High-resolution tracking of movement in the hexagonal phase

The single molecule tracking data discussed until now had an accuracy of about 20 nm. The accuracy in single-molecule localisation experiments is governed by the signal to noise ratio of the measurement.<sup>22,23</sup> Thus, by collecting more light from a single molecule one can localise it with better accuracy. However, this technique is ultimately limited by the movement of the molecules meaning that if the time required to collect the amount of light from a single-molecule to reach a certain resolution  $\Delta x$  is longer than the time that the molecule needs to move through the same distance  $\Delta x$  the actual positioning gets blurred. Thus, in order to increase the accuracy of the measurement one should increase the emitted light per unit time, *i.e.* increase the excitation power and decrease the diffusion of the molecules. An ideal material for such investigations are mesoporous structures synthesised from silica precursors and the charged template cetylhexyl-trimethylammoniumbromide (CTAB). TDI molecules incorporated into the hexagonally ordered and CTAB filled silica channels show a remarkably slow diffusion. Moreover, the use of large excitation powers ( $0.50 \text{ kW cm}^{-2}$ ) increases the emitted fluorescence intensity resulting in high-resolution single-molecule trajectories (Fig. 5). The obtained trajectories are shorter in time due to faster photobleaching, but spatial resolution down to 2–3 nm has been achieved for the brightest molecules. This is significantly below the channel-to-channel distance ( $\sim 4 \text{ nm}$  for CTAB filled channels). Therefore, it is possible to observe jumps of a molecule from one channel to one of the neighbouring channels through a local defect in the channel wall (Fig. 5a and b). Such experimentally observed trajectories reveal a local connectivity between fairly close channels. In some cases the molecule can even explore much more distant pores and thus, the analysis of such inter-channel crossings provides a direct means for a quality control of the manufactured mesoporous materials.

Additional insight can be gained about the interactions between the guest molecule and the host matrix. For instance, by inspecting the  $x(t)$  and  $y(t)$  time trajectories of a single diffusing dye molecule one can notice the presence of time intervals during which the molecule remains immobile. In Fig. 5a, for example, both  $x(t)$  and  $y(t)$  remain constant between  $t \sim 176 \text{ s}$  and  $t \sim 194 \text{ s}$ , suggesting that the molecule is immobilized (within the positioning accuracy). This means that the molecule is occasionally trapped at some sites along its trajectory; the “stop and go” movement can be understood by

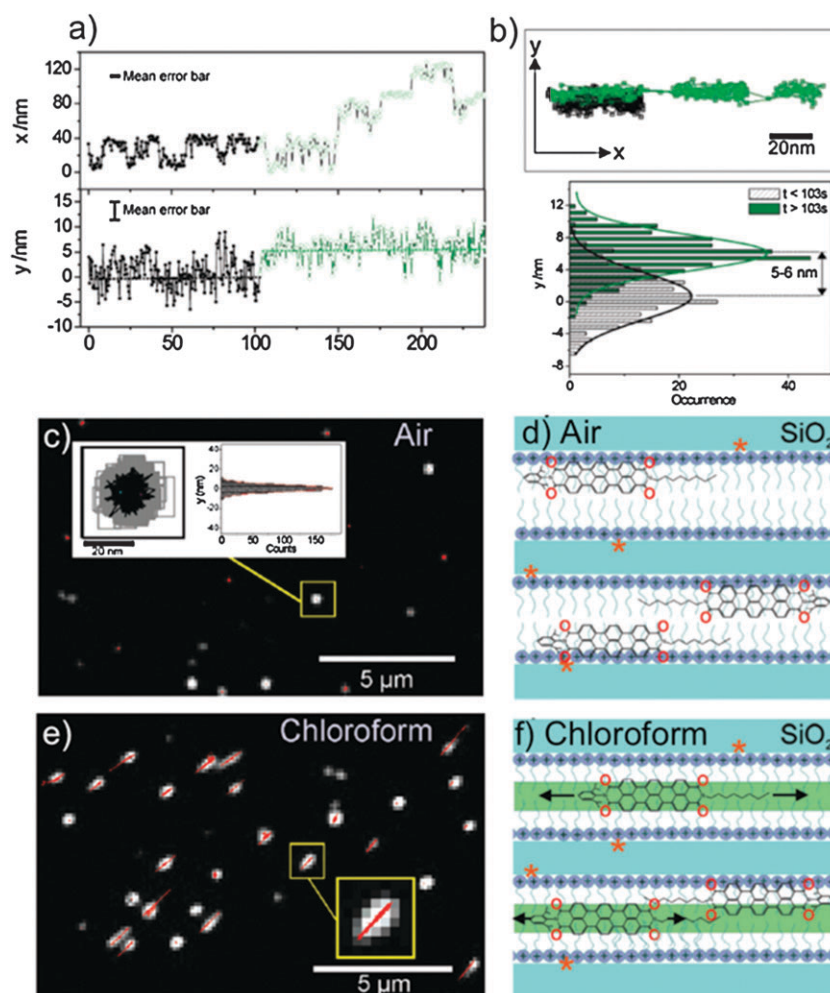


**Fig. 5** High-resolution tracking and mobility. (a) Exemplary single-molecule trajectory of a TDI molecule diffusing in long uni-dimensional CTAB filled silica channels. The main movement direction, which corresponds also to the direction of the channels is shown as  $x$ , and the direction perpendicular to it, *i.e.* the crossing from one channel to neighboring channels through local defects as  $y$ . A jump from a position (primarily) in one nano-channel to a different channel is indicated in time by a color change (black to green). (b) Two dimensional trajectory (top) and histogram of observed  $y$ -positions (bottom) for the trajectory shown in (a). (c) Diffusion in air atmosphere. The intensity distribution averaged over a long sequence of images (1000 images with 1 s integration time each) is displayed. The molecules appear as round 2-dimensional Gaussian intensity distributions (inset), thus they are completely immobilized. (d) Cartoon illustrating the observed adsorbed molecules in air atmosphere. (e) Diffusion in chloroform atmosphere. Again the intensity distribution averaged over 1000 images is shown; diffusing molecules appear as elongated objects. (f) Cartoon illustrating the diffusion in chloroform atmosphere.<sup>24</sup>

the presence of adsorption sites. Interactions with the cationic heads of the template molecules or with defect sites are two likely causes for the observed adsorption. Interestingly, it is possible to control the strength of these adsorption sites by changing environmental conditions. In an air atmosphere the adsorption to the described sites is so strong that TDI molecules are immobilized completely (Fig. 5c and d). In the presence of chloroform diffusion resumes (Fig. 5e and f), but transient interactions with adsorption sites still have an influence on the diffusion of the guest molecules. However, the strength of these interactions is reduced by the lubricant-like behavior of chloroform, and therefore the TDI molecules are only occasionally immobile. Such an adsorption could occur if the TDI molecules escape from the shell of chloroform and interact directly with the charged head groups of CTAB.

In order to quantitatively evaluate the influence of the adsorption sites on the diffusion in the presence of chloroform a statistical analysis of the linear trajectories of the diffusing molecules can be performed (Fig. 6). A first intuitive and straightforward model for the diffusion in such linear pores is a 1D random diffusion along the  $x$ -axis, *i.e.* along the direction of the channels. As will become clear, the analysis of this diffusion is best based on the cumulative probability distributions of the squared displacements. Compared with the standard method of the Mean-Square Displacement (MSD), the use of the cumulative probability distributions greatly increases the information of mobility studies, and therefore more complex behavior can be revealed, such as the effect of local heterogeneities within the sample. Fig. 6a shows the probability distribution of the squared displacements where the probability of every step is plotted against the squared

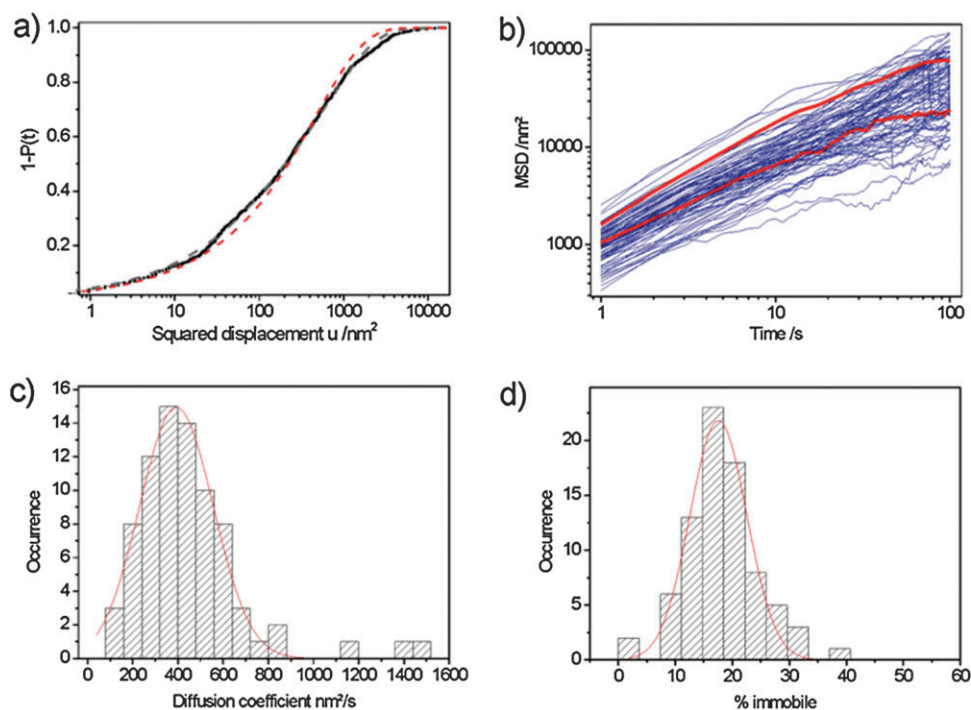


**Fig. 6** Statistical analysis of diffusion and adsorption. (a) Cumulative probability distribution of squared displacement of a single molecule trajectory for 1 s lag time. The best fit using a single diffusion coefficient (red dashes) does not describe the data well. Instead a model using pauses and diffusion (gray dashes) captures the details of the molecules diffusion. (b) MSD of observed single molecular diffusion for different molecules within a sample. The observed heterogeneity of diffusion coefficients reflects the heterogeneity of the sample. (c) Distribution of observed diffusion coefficients as computed from the single-molecule tracking analysis of 80 different molecules. (d) Distribution of time spent at adsorption sites for the analysed single molecules.<sup>24</sup>

step-size for time lags of 1 s. It is obvious that a 1D random walk model (fit shown by red, dashed line) is not an accurate enough model to describe the observed diffusion. The gray dashed line shows the fit using a linear combination of a 1D random walk and a second term which takes into account the presence of adsorbed states, describing the data better (chi-squared is 8-fold reduced). From the fit one obtains the percentage of the time that the TDI is immobilized at adsorption sites (13%). The same procedure can be applied to different time delays (2 s, 3 s, ...) in order to test whether the behaviour is similar over different time-scales. In addition in order to obtain a better understanding of the local heterogeneities of the sample, one typically performs such analysis for a large number of different single molecule trajectories (Fig. 6b). One finds that most of the molecules show a behaviour that is not perfectly linear with time as would be expected for a normal random walk. Instead the observed MSD is slightly curved for high time values. This indicates the presence of a confined diffusion, which is consistent with the presence of “dead ends” in the channel, *i.e.* similar local defects than the aforementioned connections between neighbouring channels. Moreover, from the initial slope of the MSD plots it is possible to calculate the diffusion coefficient for each molecule. The distribution of the diffusion coefficients for many molecules resembles a Gaussian with a mean diffusion coefficient of  $390 \text{ nm}^2 \text{ s}^{-1}$  (Fig. 6c). Moreover, the histogram of the percentage of adsorption time per trajectory also follows a Gaussian distribution with a maximum at 18% of the time, which means that a molecule spends on average

18% of its walk immobilized at an adsorption site. An additional interesting observation is that the distributions are both really broad which denotes the presence of large heterogeneities within the sample.<sup>24</sup>

### Characterization of adsorption sites

The interactions between the fluorescent probe and its immediate environment in the confinement regions can be described in more detail by investigating simultaneously the molecule's orientation and emission spectrum.<sup>25,26</sup> The emission spectrum is an extremely sensitive measure because small changes in the host-guest interactions result in a detectable change in the spectrum. Additionally the orientation of the dye molecule gives a good indicator about the local sample geometry. Since the size of TDI molecules is large compared to the channel diameter of CTAB templated mesoporous hexagonally ordered silica channels, the rotation about one of its axis is prevented. As a result, the orientation of the TDI molecule incorporated into the channel maps the orientation of the channel. A change in a molecule's orientation is determined by a change in the polarisation of its emitted fluorescent light indicating a small movement and/or local re-arrangement. In the case of CTAB templated mesoporous films individual molecules can diffuse within confined regions for tens of minutes. Therefore, by placing the detection volume of a confocal microscope directly on the molecule's position one observes the molecule's local dynamics with high temporal resolution. Fig. 7 shows the time evolution of orientation and

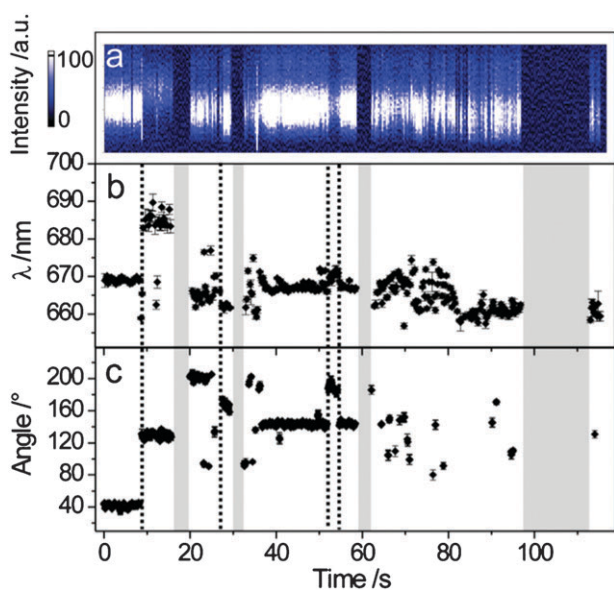


**Fig. 7** Spectral and polarisational dynamics at adsorption sites. (a) Time-series of recorded fluorescence emission spectra of a single TDI molecule embedded into a hexagonally ordered mesoporous silica film filled with CTAB. (b) Time series of the extracted wavelength of the emission maximum. Grey bars denote time-periods where no sufficient single-molecule fluorescence signal was detected, since the molecule went into a dark state. (c) Determined angle of the transition-dipole of the single molecule. In addition to time periods where no sufficient fluorescence was detected to determine the polarization of the dye molecules (grey bars), also time-intervals with rapidly rotating polarization were detected, indicated by missing orientational data-points.<sup>26</sup>

emission spectra for a single TDI molecule within a confined region. The intensity chart in Fig. 7a displays the raw sequence of spectra. Fig. 7b and c show the central position of the emission maximum and the corresponding orientation of the molecule, respectively. Periods of stable fluorescence are sometimes interrupted transiently by dark states, so called blinking events. The blinking events noted as grayed-out areas in the graph are typical signatures of individual emitters. One can observe periods of long stable orientations and occasional abrupt orientational jumps as well as other times when the molecule is undergoing fast re-orientation dynamics that were interrupted by short periods during which it shows a stable orientation. Interestingly, the spectral trajectory (Fig. 7b) shows dynamics which are clearly correlated with the orientational trajectory with the following characteristics: Firstly, each time a molecule remains at a stable orientation it also shows a specific stable fluorescence spectrum. Secondly, an orientational jump is accompanied by a spectral jump. The coinciding periods of constant orientation and constant spectrum indicate that the molecule was neither re-orienting nor did its immediate vicinity change. The interpretation of these observed effects is that localized interactions between the dye molecule and the host material caused the molecule to become adsorbed at specific sites in the material. The duration of these periods reflect the strength with which the molecule was adsorbed to a site. More rarely it is also observed that the fluorescence emission spectrum of the molecule changes without an accompanying change in the polarisation signal.

This effect can be explained by changes in the local environment of the molecule such as changes in the local charge distribution.

### Controlling the adsorption sites

As already discussed above, the strength of the adsorption site can be altered by varying the atmosphere: chloroform or water act as lubricants thus decreasing the strength of the adsorption sites.<sup>24</sup> In addition it is also possible to alter the strength of the adsorption sites by chemically shielding them.<sup>27</sup> To this end one can investigate the diffusion in mesoporous materials that are made using various amounts of covalently modified silica precursor materials (Fig. 8). For example by attaching an alkyl chain adsorption sites are effectively shielded and the observed diffusion coefficient increases with increasing functionalisation density as well as with increasing alkyl chain length. In contrast when the silica walls are modified with phenyl groups, a more complex behaviour is observed. While at low functionalisation densities the observed diffusion coefficients are higher than those of the unfunctionalised mesoporous silica, an increase in functionalisation density decreases the observed diffusion coefficient. This can be explained by two competing processes. At the lowest functionalization density the bulky and rigid phenyl groups effectively shield the surface adsorption sites. In fact at these low functionalisation densities (2.5%) the shielding is superior to that of alkyl chains. The decreasing mean diffusion coefficient with increasing functionalization density can be explained by attractive pi-pi interactions between the rigid phenyl groups and the aromatic system of the dye or the phenyl groups at both ends of the dye. Due to the diisopropyl groups in the dye, these end groups are twisted out of the aromatic plane of the dye. This is sterically advantageous for interactions with the phenyl functionality. The capability to control the strength of the adsorption sites, and ultimately the diffusion coefficient  $D$  of the guest molecules, has enormous potential for future applications of mesoporous materials, *e.g.* in the field of catalysis or controlled drug release from mesoporous silica particles.<sup>7</sup>

### Summary and outlook

The increasing ability to orient mesostructured materials on a macroscopic length scale opens the possibility to exploit the organization of mesoporous solids for applications in which ordered, anisotropic, or even monolithic structures are required. Promising applications include separations, catalysis, chemical sensors, and host-guest chemistry. The methodology presented, namely the investigation of diffusion of single-molecules within the pores of the mesoporous films, is a valuable tool to characterize large structured areas of such mesoporous films. By overlaying TEM images and single molecule trajectories it becomes possible to investigate how domain structure influences the local diffusional properties of the guest molecules. While in TEM images large homogeneous areas are oftentimes observed, the diffusion of single molecules in such domains is vastly heterogeneous. Single-molecule analysis allows to investigate these heterogeneities in great detail revealing local adsorption sites, as well as point defects where the molecule's pathway is obstructed,

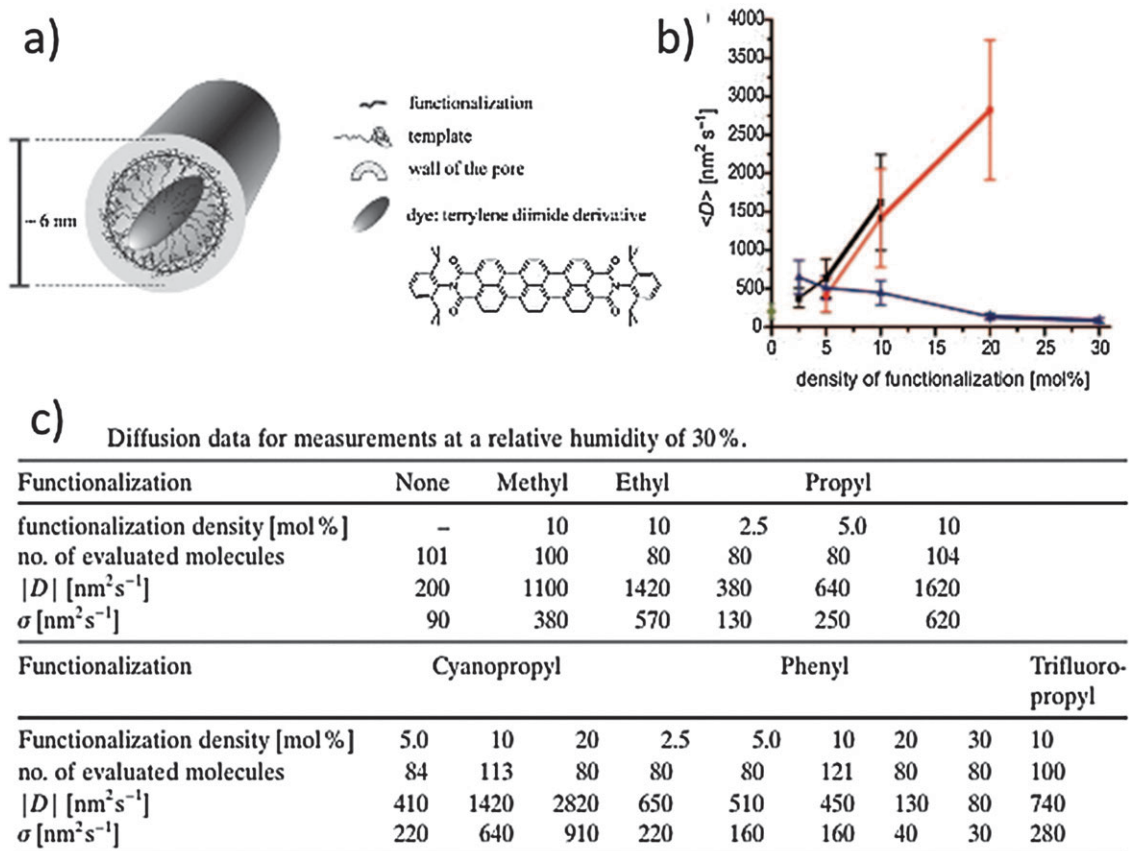


**Fig. 8** Modifying adsorption rates. (a) Cartoon of the TDI-molecule incorporated into a mesoporous silica channel with modified silica walls. All dimensions are drawn approximately to scale. (b) Observed diffusion coefficients for different functionalisations as a function of functionalisation density (black: propyl, red: cyano-propyl, blue: phenyl, green: unfunctionalised). (c) Table reviewing the observed effects of different functionalisations/densities on  $D$ .<sup>27</sup>

thus causing it to turn around, or wall openings which lead to a diffusion perpendicular to the pore geometry. The details about the host–guest interactions revealed by the single molecule analysis allow for the controlled modification of channel surfaces and thus ultimately for a tailored design of nanometre sized channels. Important control parameters include the size, shape and chemical nature of the guest molecules, as well as modifications of the channel walls, allowing for a control of diffusion constants of guest molecules within the host material both locally as well as globally. This will be extremely important for using these highly promising materials in advanced catalysis applications.

## Acknowledgements

The authors wish to acknowledge financial support by the Nanosystems Initiative Munich (NIM), the Center for Integrated Protein Science Munich (CIPSM) and the Sonderforschungsbereich 486 and 749. The authors thank Klaus Müllen and Thomas Bein for the long-term productive collaboration and all laboratory members that contributed to the original publications.

## References

- N. K. Raman, M. T. Anderson and C. J. Brinker, *Chem. Mater.*, 1996, **8**, 1682–1701.
- S. Polarz and B. Smarsly, *J. Nanosci. Nanotechnol.*, 2002, **2**, 581–612.
- S. Polarz and A. Kuschel, *Chem.–Eur. J.*, 2008, **14**, 9816–9829.
- F. Laeri, F. Schüth, U. Simon and M. Wark, *Host–Guest-Systems Based on Nanoporous Crystals: Synthesis, Properties and Applications*, ed., Wiley VCH, Weinheim, 2003.
- V. Rebbin, R. Schmidt and M. Froba, *Angew. Chem., Int. Ed.*, 2006, **45**, 5210–5214.
- D. E. De Vos, M. Dams, B. F. Sels and P. A. Jacobs, *Chem. Rev.*, 2002, **102**, 3615–3640.
- T. Lebold, C. Jung, J. Michaelis and C. Brauchle, *Nano Lett.*, 2009, **9**, 2877–2883.
- A. Schlossbauer, J. Kecht and T. Bein, *Angew. Chem., Int. Ed.*, 2009, **48**, 3092–3095.
- D. J. Cott, N. Petkov, M. A. Morris, B. Platschek, T. Bein and J. D. Holmes, *J. Am. Chem. Soc.*, 2006, **128**, 3920–3921.
- J. V. Kärger, R. Valiullin and S. Vasenkov, *New J. Phys.*, 2005, **7**, 1–15.
- Single Molecule Optical Detection, Imaging and Spectroscopy*, ed. T. M. Basche, W. E. Moerner, M. Orrit and U. P. Wild, VCH, 1996.
- R. M. Dickson, D. J. Norris, Y. L. Tzeng and W. E. Moerner, *Science*, 1996, **274**, 966–969.
- W. E. Moerner, *Science*, 1994, **265**, 46–53.
- Single Particle Tracking and Single Molecule Energy Transfer*, ed. C. Brauchle, D. C. Lamb and J. Michaelis, Wiley-VCH, Weinheim, 2009.
- G. Seisenberger, M. U. Ried, T. Endress, H. Buning, M. Hallek and C. Brauchle, *Science*, 2001, **294**, 1929–1932.
- C. J. Brinker, Y. F. Lu, A. Sellinger and H. Y. Fan, *Adv. Mater.*, 1999, **11**, 579–585.
- F. O. Holtrup, G. R. J. Muller, H. Quante, S. Defeyter, F. C. DeSchryver and K. Müllen, *Chem.–Eur. J.*, 1997, **3**, 219–225.

- 
- 18 C. Jung, N. Ruthardt, R. Lewis, J. Michaelis, B. Sodeik, F. Nolde, K. Peneva, K. Mullen and C. Brauchle, *ChemPhysChem*, 2009, **10**, 180–190.
- 19 C. Jung, B. K. Müller, D. C. Lamb, F. Nolde, K. Müllen and C. Bräuchle, *J. Am. Chem. Soc.*, 2006, **128**, 5283–5291.
- 20 J. Kirstein, B. Platschek, C. Jung, R. Brown, T. Bein and C. Brauchle, *Nat. Mater.*, 2007, **6**, 303–310.
- 21 F. Feil, C. Jung, J. Kirstein, J. Michaelis, C. Li, F. Nolde, K. Müllen and C. Brauchle, *Microporous Mesoporous Mater.*, 2009, **125**, 70–78.
- 22 T. Schmidt, G. J. Schutz, W. Baumgartner, H. J. Gruber and H. Schindler, *Proc. Natl. Acad. Sci. U. S. A.*, 1996, **93**, 2926–2929.
- 23 A. Yildiz, J. N. Forkey, S. A. McKinney, T. Ha, Y. E. Goldman and P. R. Selvin, *Science*, 2003, **300**, 2061–2065.
- 24 C. Jung, J. Kirstein, B. Platschek, T. Bein, M. Budde, I. Frank, K. Mullen, J. Michaelis and C. Brauchle, *J. Am. Chem. Soc.*, 2008, **130**, 1638–1648.
- 25 C. Jung, C. Hellriegel, B. Platschek, D. Wohrle, T. Bein, J. Michaelis and C. Brauchle, *J. Am. Chem. Soc.*, 2007, **129**, 5570–5579.
- 26 C. Jung, C. Hellriegel, J. Michaelis and C. Brauchle, *Adv. Mater.*, 2007, **19**, 956–960.
- 27 T. Lebold, L. A. Muhlstein, J. Blechinger, M. Riederer, H. Amenitsch, R. Kohn, K. Peneva, K. Mullen, J. Michaelis, C. Brauchle and T. Bein, *Chem.–Eur. J.*, 2009, **15**, 1661–1672.
- 28 A. Zürner, J. Kirstein, M. Dobliger, C. Brauchle and T. Bein, *Nature*, 2007, **450**, 705–709.
- 29 J. Kirstein, Doctoral Thesis, Ludwig-Maximilians-University, Munich, 2007.